Practical Course III

Circuit Quantum Electrodynamics

Otto T.P. Schmidt

November 24, 2021

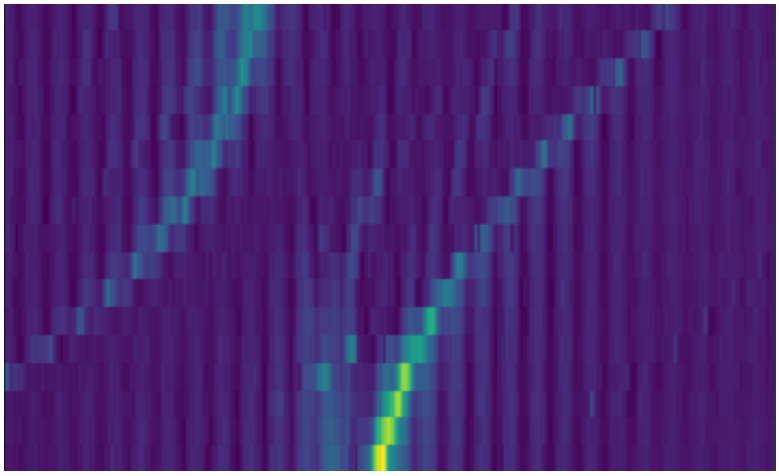

Abstract

Two-level quantum systems are the fundamental logical unit of quantum computing. However, the quantum states need to be controlled for any quantum computation.
This experiment introduces a possible realisation of such a controlled two-level regime, the circuit quantum electrodynamics (CQED). Instead of using an atom as quantum object, CQED establishes a two-level system by creating an artificial atom through electrical circuits.
In this construction two systems interact with each other, a cavity and the circuit (to which we will refer as qubit).
After an analysis of the cavity, we will inspect the interaction of the systems cavity and qubit and derive the coupling strength for a set of parameters.

Contents

1 Introduction **4**

2 Quantum Information Theory **5**

2.1 Transmon 5

2.1.1 Josephson Junction 6

2.1.2 Tunability and SQUID loop 8

2.2 Jaynes-Cummings model 9

2.2.1 Dispersive and resonant regime 10

3 Experimental setup **12**

3.1 Qubit-cavity system 12

3.2 Cryogenic dilution refrigerator 12

4 Data analysis **14**

4.1 Cavity spectroscopy 14

4.1.1 Observations 15

4.1.2 Analysis 17

4.2 Coil sweep 18

4.2.1 Observations 19

4.2.2 Analysis 21

5 Conclusion **28**

Appendices **29**

A Appendix A **29**

B Appendix B **29**

B.1 Shortest distance 29

B.2 Avoided crossing 31

1 Introduction

Quantum computing is all about controllability. We therefore need to understand the interaction of a 3D microwave cavity and a qubit. For this we need a measure of interaction of both systems, the coupling strength g.
In classic quantum electrodynamics (i.e. cavity QED), the coupling strength describes the atom-photon interaction. However, the stability and controllability of atoms is small compared to modern artificial atoms, namely superconducting two-level circuits. Therefore, for the system at hand, the coupling strength quantizes the interaction of the cavity and the superconducting qubit.

The first part of this experiment will consist in the analysis of the uncoupled cavity. The main goal is to determine the difference of the resonance frequency between the bare, uncoupled and the coupled cavity.
After the cavity is characterized we can proceed to the main part, the estimation of g. For different input powers of the signal we will tune the system with an external magnetic field and observe the transmitted frequencies. A suitable Hamiltonian for the two-level system will then introduce the coupling strength.
The following data analysis will illustrate and discuss the findings.

2 Quantum Information Theory

In order to understand the results of the experiment, a brief outline of the technical realisation of the qubit and coupled system and its quantum mechanical description will be given.

2.1 Transmon

A qubit is a fundamental quantum system. The most basic notation of this quantum mechanical form of the bit is:

$$|\psi\rangle = \alpha\,|g\rangle + \beta\,|e\rangle \tag{1}$$

Here the states $|g\rangle$ and $|e\rangle$ represent a ground and excited state of the system and $|\alpha|^2+|\beta|^2 = 1$.

This qubit is technically realised by a construction of various superconducting circuits including inductors, capacitors and a Josephson junction. It is therefore an intricate system of different parts. In this particular setup we use a transmon qubit (**t**ransmission **l**ine **s**hunted **p**lasma **o**scillation qubit)[10] which is placed inside a 3D copper cavity.

In principle the transmon is a quantized anharmonic oscillator, i.e. an oscillator with non-equidistant energy levels. Such an oscillator can be constructed by means of an LC-circuit where the nonlinear inductor is a Josephson junction.[10]
In classical electronic notation the Hamiltonian of a classical LC circuit is

$$H_{LC} = \frac{Q^2}{2C} + \frac{\Phi^2}{2L} \tag{2}$$

where Q is the charge on the capacitor, C the capacitance, Φ the magnetic flux of the inductor and L the inductance.
Observables correspond to linear operators in quantum mechanics. If we follow the translation from the classic mechanical to quantum electronic Hamiltonian (see Appendix A), we can define the annihilation and creation operators

$$\hat{a} = \frac{1}{\sqrt{2\hbar Z}}(Z * \hat{Q} + i\hat{\Phi})$$
$$\hat{a}^\dagger = \frac{1}{\sqrt{2\hbar Z}}(Z * \hat{Q} - i\hat{\Phi})$$

with the impedance $Z = \sqrt{L/C}$ of the circuit.
With this the quantum electronic Hamiltonian of the LC-circuit reads

$$\hat{H} = \hbar\omega(\hat{a}^\dagger\hat{a} + \frac{1}{2}) \tag{3}$$

This harmonic oscillator and its Hamiltonian define the fundamental quantum properties of the qubit. However, this system is only the basis for the transmon and needs to be adjusted.

2.1.1 Josephson Junction

Now that the Hamiltonian of the fundamental quantum system, the harmonic oscillator, has been established, the question of distinguishability of different states arises. The problem is that the energy spacing for the LC-circuit is equidistant. This makes it impossible to differentiate states. However, for the use in quantum computing precise tuning and identification of the eigenstates of the systems are necessary.
A regime with distinguishable eigenstates can be achieved if we introduce anharmonicity to the oscillator. This is possible by using a nonlinear inductor called Josephson junction.[10]
This inductor is formed by two electrodes which are separated by an insulator thin enough, such that Cooper pairs can tunnel through. Cooper pairs are coupled electrons that form a boson. For low temperatures the Cooper pairs are responsible for superconductivity.
The Josephson junction introduces the desired anharmonicty via the so called Josephson inductance

$$L_J = \frac{\Phi_0}{2\pi I_C} \frac{1}{cos(\delta)} \tag{4}$$

where $\Phi_0 = h/2e$, I_C is the critical current of the junction and $\delta = \frac{2\pi\Phi(t)}{\Phi_0}$ with the magnetic flux $\Phi(t)$.
The energy of the inductor is (Josephson energy):

$$E_J = \frac{I_C\Phi_0}{2\pi} cos(\delta) = E_{J_0} cos(\delta) \tag{5}$$

The Hamiltonian of the LC circuit is given in eq. 2. This can be written as the Hamiltonian operator

$$\hat{H}_{LC} = 4\frac{e^2}{2C}\hat{n}^2 + (\frac{\Phi_0}{2\pi})^2 \frac{\hat{\delta}}{2L} \tag{6}$$

by using $\hat{\delta} = 2\pi\hat{\Phi}/\Phi_0$ and $\hat{n} = \hat{Q}/2e$ (excess number of Cooper pairs).
If the linear inductivity is now exchanged with the Josephson inductivity L_J we get:

$$\hat{H}_{LC} = 4\frac{e^2}{2C}\hat{n}^2 - E_J cos(\hat{\delta}) \tag{7}$$

Since equations 2 and 6 need to correspond, we have

$$\hat{\delta} = 2\sqrt{\mu}(\hat{a} + \hat{a}^\dagger)$$
$$\hat{n} = \frac{\hat{a} - \hat{a}^\dagger}{4i\sqrt{\mu}}$$

where $\mu = \sqrt{E_C/8E_J}$ with $E_J = 2\pi\Phi_0 I_C$ the energy stored in the junction for no external flux and $E_C = e^2/2C$ is the energy stored in the capacitor.[7][4]

With perturbation theory we find for the first two energy states [4]

$$E_1 = \hbar\omega_q(\frac{1}{2} + \frac{1}{4}\mu - \frac{3}{8}\mu^2)$$
$$E_2 = \hbar\omega_q(\frac{3}{2} - \frac{5}{4}\mu - \frac{27}{8}\mu^2)$$

with $\omega_q = \sqrt{8E_C E_J}/\hbar$.

From these deductions we can see how the energy spacing are non-equidistant.

2.1.2 Tunability and SQUID loop

From equation 5 above we can see how the Josephson energy depends on an external magnetic flux. By connecting two Josephson inductors in parallel, the reactivity of the Josephson energy on the external flux is greatly increased [10]. Therefore only small magnitudes of magnetic flux need to be applied to vary E_J. The parallel wiring is called a SQUID (superconducting quantum interference device). This extended version of an LC circuit is called transmon (see fig. 1)

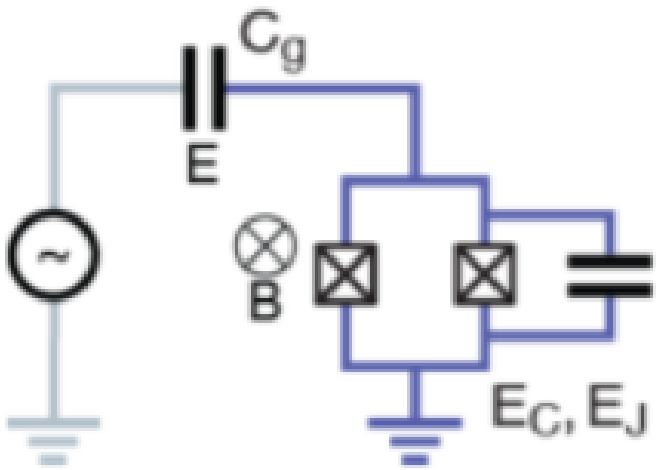

Figure 1: Circuit of a transmon with energies E_C and E_J and capacity C_g. The external magentic field is denoted with B.[10]

The external flux also affects the qubit transition frequency $\omega_q = \sqrt{8E_C E_J(\Phi(t)}/\hbar$ with $E_C \approx$ 0.3 GHz and $E_J(\Phi) = E_{J,max}|cos(\pi\Phi/\Phi_0)|$. Here E_J is the Josephson energy for the SQUID and $E_{J,max} \approx 20$ GHz.[3]
With this relation we can tune the relative frequency between the qubit and the cavity via the external magnetic flux.

2.2 Jaynes-Cummings model

The interaction of light with a two-level system, i.e. the transmon, and the resonant modes of the copper cavity is aptly described with the Jaynes-Cummings Hamiltonian.[11]
The operators of a two-level system can be depicted through Pauli matrices such that the qubit state Hamiltonian enters the model as

$$\hat{H}_Q = \frac{\hbar\omega_q}{2}\sigma^+\sigma^- = \frac{\hbar\omega_q}{2}\sigma_z \tag{8}$$

with $\sigma^+ = |e\rangle\langle g|$ and $\sigma^- = |g\rangle\langle e|$ the raising and lowering operators of the qubit (i.e. $\sigma^+|g\rangle = |e\rangle$ and $\sigma^-|e\rangle = |g\rangle$) and ω_q the transition frequency of the qubit. The ground state has $E = 0$, the excited state $E = \hbar\omega_q/2$. The operators $\hat{a}^\dagger$, $\hat{a}$ of the basic LC-circuit are incorporated in these new operators.
The Hamiltonian of a cavity mode with frequency ω_r is described by an harmonic oscillator

$$\hat{H}_C = \hbar\omega_r\hat{a}^\dagger\hat{a} \tag{9}$$

Therefore the energy eigenvalues of the cavity are $E_C = \hbar\omega_r n$ with n the number of photons in the cavity.
The Jaynes-Cummings Hamiltonian captures the interaction of cavity and qubit with an additional coupling term. This coupling Hamiltonian reads

$$\hat{H}_I = \hbar g(\hat{a}\sigma^+ + \hat{a}^\dagger\sigma^-) \tag{10}$$

The two terms formulate an interaction type of cavity and qubit, i.e. the periodic information exchange between qubit and cavity at rate g. The first term $\hat{a}\sigma^+$ refers to the annihilation of a photon and simultaneous excitation of the qubit whereas $\hat{a}^\dagger\sigma^-$ describes the relaxation of the qubit into the ground state and creation of a photon.
Combining the three parts we obtain the full Jaynes-Cummings Hamiltonian:

$$\hat{H}_{JC} = \hbar\omega_r\hat{a}^\dagger\hat{a} + \frac{\hbar\omega_q}{2}\sigma^+\sigma^- + \hbar g(\hat{a}\sigma^+ + \hat{a}^\dagger\sigma^-) \tag{11}$$

For the general product states $|n,\ g\rangle$ and $|n-1,\ e\rangle$ of the coupled system, we can formulate the matrix representation of the Jaynes-Cummings Hamiltonian [11]

$$\hat{H}_{JC} = \begin{pmatrix} \hbar\omega_r n & \hbar g\sqrt{n} \\ \hbar g\sqrt{n} & \hbar(n\omega_r + \omega_q) \end{pmatrix} \tag{12}$$

The eigenstates of this Hamiltonian are called dressed states and read [8]

$$|n,+\rangle = sin(\theta_n/2)\,|n,g\rangle + cos(\theta_n/2)\,|n-1,e\rangle$$
$$|n,-\rangle = cos(\theta_n/2)\,|n,g\rangle - sin(\theta_n/2)\,|n-1,e\rangle$$

with θ_n from $tan(\theta_n) = 2g\sqrt{n}/\Delta$ and eigenenergies

$$E_{\pm,n} = \hbar\omega_r n \pm \frac{\hbar}{2}\sqrt{4g^2 n + \Delta^2} \tag{13}$$

Here $\Delta = \omega_r - \omega_q$ denotes the detuning between the cavity and the qubit.
In this setup we reach the strong coupling condition which assumes that $\gamma,\ \kappa \ll g$ (with γ the atomic decay rate and κ the cavity decay rate)[2]. This means that the atomic system can absorb and re-emit a given photon many times before it leaks from the cavity or is spontaneously emitted. In this regime the Jaynes-Cummings model is fully realized.

2.2.1 Dispersive and resonant regime

In the analysis of possible quantum states of the combined system we need to distinguish between the case where $\Delta \approx 0$ and where $g/\Delta \ll 1$. The first case is called the resonant regime, the second dispersive.
The above defined Jaynes-Cummings Hamiltonian describes the eigenenergies in the resonant regime.
For the resonant regime we therefore have:

$$\Delta E = E_{+,n} - E_{-,n} = 2\hbar g\sqrt{n} \tag{14}$$

The schematic anti-crossing of frequencies corresponding to the energy split in eq. 14 can be seen in figure 2 below.

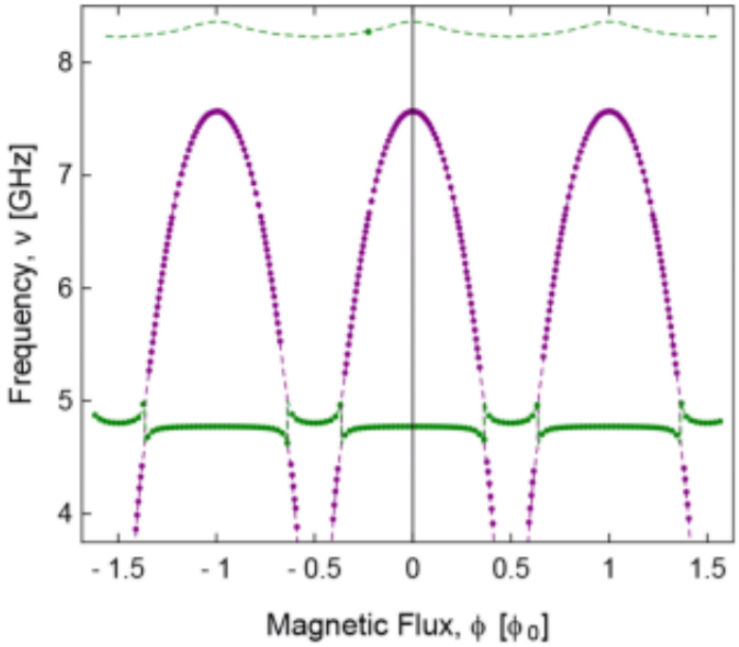

Figure 2: Dependence of the frequencies of the coupled qubit-cavity system on an external magnetic flux Φ. The cosine priodicity of the Josephson energy can be seen. The qubit frequency is marked with purple dots, the cavity frequency with green dots.

A schematic of the energy levels for a resonant coupled qubit-cavity system is shown below.

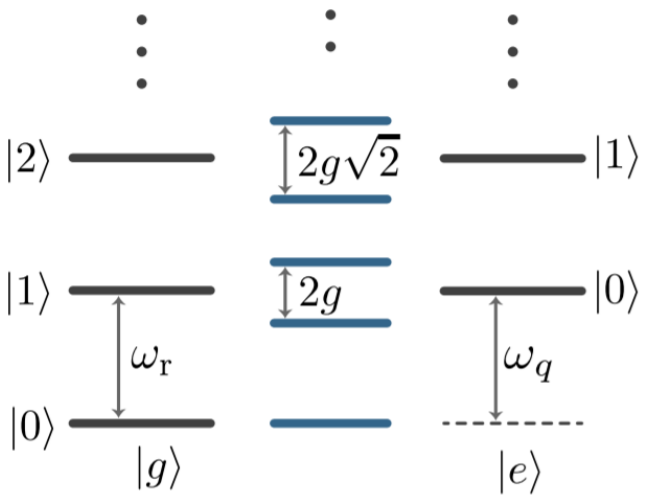

Figure 3: Energy spectrum of the Jaynes-Cummings Hamiltonian for uncoupled (grey) and coupled (blue) qubit-cavity system. The number of photons is given with $|n = 0, 1, 2, ...\rangle$.[1]

In the dispersive regime the Hamiltonian changes. Since all measurements were taken in the avoided crossing region of the system, the dispersive regime and its Hamiltonian will not be outlined. A discussion of both the resonant and dispersive regime is given in [1].

3 Experimental setup

The experimental setup consisted of two main parts that remained unchanged throughout the experiment. These parts will be briefly outlined in the following sections.
The results from different measurements were acquired using a *LabView*-based measurement framework.

3.1 Qubit-cavity system

The core of the setup is the qubit-cavity system. Here a small chip containing the transmon circuit (see section 2.1.2) was placed in the center of a copper cavity. Through an input microwaves were sent into the cavity. The resonant frequencies were then read out by an output.
Figure 4 shows the cavity and transmon chip.

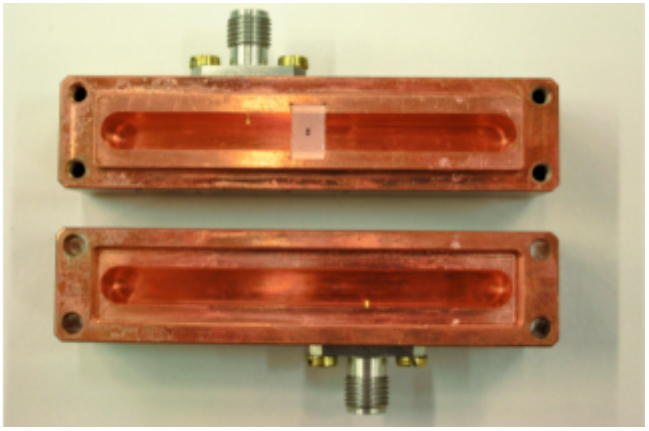

Figure 4: The open cavity. The silver input and output ports are visible on top and bottom of the cavity. The chip containing the transmon circuit is placed in the center (transparent square in the upper cavity half).[6]

3.2 Cryogenic dilution refrigerator

Superconductivity is a main aspect to control a quantum system. It is crucial since the internal electrical resistance of a circuit increases the signal decay.
This causes problems since prepared quantum states of the transmon circuit may dissipate and decay before a measurement can be conducted.
It is therefore of paramount importance to reduce the signal decay and thereby increase the

coherence time of a state.

This is achieved if the qubit-cavity system is put into the superconducting regime where the resistance is negligible small.

Technically this was realised by using a dilution refrigerator that cools down the sample to approx. 30 mK using a bath of liquid helium.

4 Data analysis

The experimental setup has been described in section 3. For the different experimental runs different parameter sweeps and resolutions have been used.
Two different experiments were conducted:

1. Cavity spectroscopy: in order to obtain the characteristics of the coupled system of qubit and cavity as well as the uncoupled cavity, a sweep of the input microwave frequency was made for a fixed external voltage.

2. Coil sweep: since the qubit's transition frequency changes with an externally applied magnetic flux (see section 2.1.2), we can use a sweep in input frequency and coil voltage (changes with magnetic flux) to observe how the readout energy in the resonant regime changes. We will conduct a series of these two dimensional sweeps with different input power and analyse the result to obtain an estimate for the coupling strength g.

4.1 Cavity spectroscopy

For this analysis the coil voltage was set to 0 V. At this constant voltage the qubit transition frequency should not change (see section 2.1.2). However, the amplitude of the input signal was changed. From equation 9 we can see how the amount of photons inside the cavity changes the energy of the coupled system.
The conversion from signal amplitude to decibel (dB) is:
Amplitude setting in *LabView* (x) to voltage (V):

$$V(x) = A * (\frac{4x10^{-3}}{0.15}) * C \tag{15}$$

with $A = 1$ the input wave parameter and $C = 0.75$ V the output range.
Voltage (v) to decibel (D):

$$D(v) = 10 * \log_{10}(\frac{(\frac{v}{\sqrt{2}})^2}{50 \times 10^{-3}}) \tag{16}$$

With this we can obtain the power of the signal in Watt (W):

$$W(D) = 10^{\frac{D-30}{10}} \tag{17}$$

4.1.1 Observations

A series of frequency sweeps from 6.4 GHz to 6.53 GHz at coil voltage $V = 0$ was conducted for various input amplitudes. The sampling frequency was 1.75 MHz. Each data point is obtained by averaging 10000 repeated acquisitions.

In order to properly identify possible resonant frequencies the fit to a Lorentzian is necessary. The single Lorentzian fit function reads:

$$f(\nu) = \frac{A\sigma^2}{((\nu - \nu_0)^2 + \sigma^2)} + C \tag{18}$$

Here A is an amplitude, ν_0 the center frequency, σ the width of the peak and C an offset. Similarly the fitting function for a twofold Lorentzian reads:

$$f_{multi}(\nu) = \frac{A_1\sigma_1^2}{((\nu - \nu_{0,1})^2 + \sigma_1^2)} + \frac{A_2\sigma_2^2}{((\nu - \nu_{0,1})^2 + \sigma_2^2)} \tag{19}$$

Here again A_i is an amplitude, $\nu_{0,i}$ the center frequency and σ_i the width of the peak with i the index of the i-th peak. The left peak with index $i = 1$, the right one with $i = 2$.

The observations of the frequency sweeps for different input power are given in the following figures. For two observations (fig. 8a and 8b) a suitable Lorentzian fit was applied.

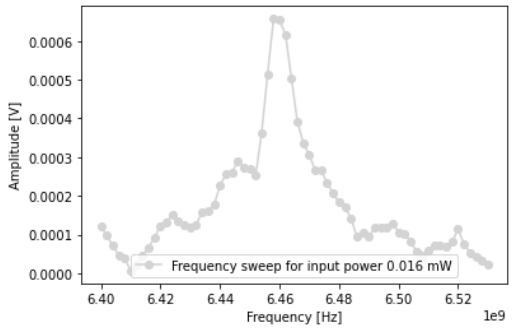

Figure 5: Sweep for input power 16.03 µW

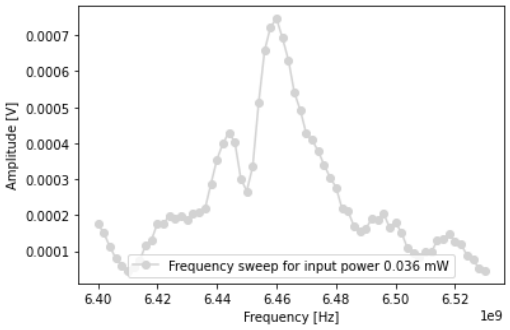

Figure 6: Sweep for input power 36.3 µW

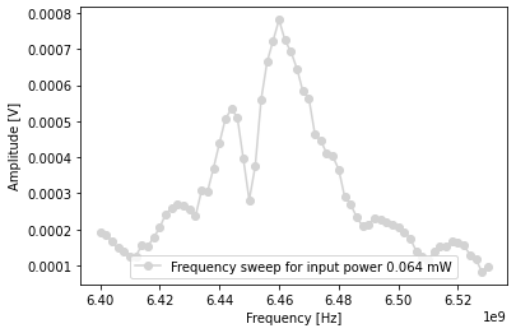

Figure 7: Sweep for input power 64.12 µW

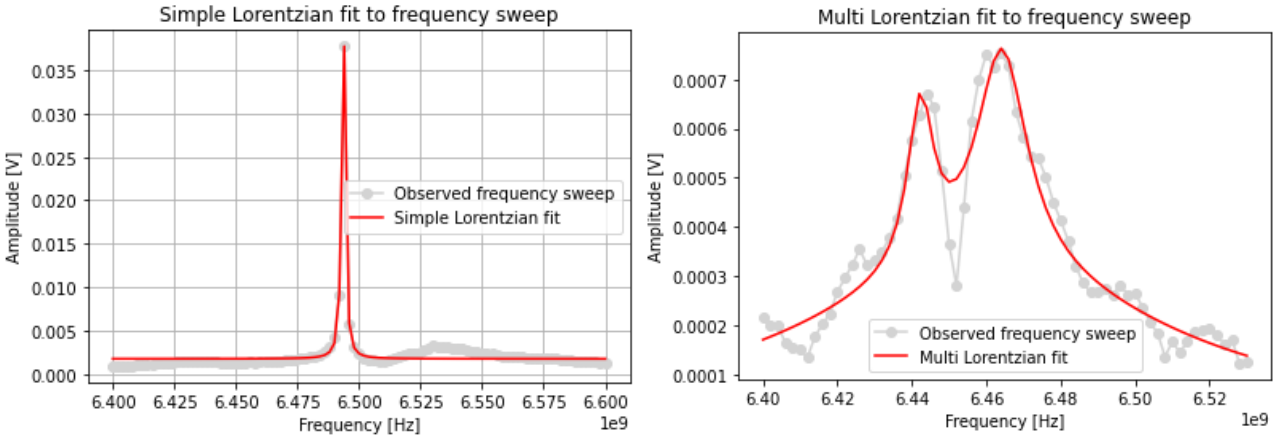

(a) Frequency sweep for 1.6 mW

(b) Frequency sweep for 100 µW

Figure 8: Simple and multi Lorentzian fits for different input power.

The parameters for the simple Lorentzian fit (fig. 8a) are given below in table 1.

Table 1: Values and standard deviations for the fitting parameters ν_0 and σ for the function $f(\nu)$ in equation 18

ν_0 [Hz]	σ [Hz]
$(6.493 \times 10^9 \pm 7.803 \times 10^4)$	$(7.589 \times 10^5 \pm 7.518 \times 10^4)$

Similarly, table 2 shows the parameters and errors for the multi Lorentzian fit shown in fig. 8b.

Table 2: Values and standard deviations for the fitting parameters A_i, $\nu_{0,i}$ and σ_i for the function $f(\nu)$ in equation 19.

A_1 [a.u.]	$\nu_{0,1}$ [Hz]	σ_1 [Hz]
$(3.340 \times 10^{-4} \pm 4.609 \times 10^{-5})$	$(6.442 \times 10^9 \pm 5.321 \times 10^5)$	$(4.214 \times 10^6 \pm 1.060 \times 10^6)$
A_2 [a.u.]	$\nu_{0,2}$ [Hz]	σ_2 [Hz]
$(4.507 \times 10^{-4} \pm 5.700 \times 10^{-5})$	$(6.464 \times 10^9 \pm 5.839 \times 10^5)$	$(8.413 \times 10^6 \pm 1.658 \times 10^6)$

4.1.2 Analysis

The presented observations bear some insights into the coupled system. Although no voltage is applied, the qubit still affects the readout frequency since the observations show not only one resonance frequency of the cavity but some additional interaction. The illustration 2 shows how cavity and qubit interact in general. Figure 2 therefore suggests a multi-modality (i.e. the two peaks in figures 6, 7 and 8b) in the avoided crossing region.

Before an analysis of the observations can be conducted, the regime of the system has to be known. The distinction between resonant and dispersive regime has been made in section 2.2.1. For the value $V = 0$ cavity and qubit seem to be in the resonant regime since for $V = 0$ the system is in the avoided crossing region (see section 4.2 and fig. 9). With this assumption the observations can be properly analysed.

The graphs 5, 6, 7 and 8b show cavity-qubit interaction. In the resonant regime there seems to exist a second resonance frequency which increases for higher input power. This becomes most prominent in fig. 8b: there is a left peak, centered around $\nu = 6.442$ GHz, and a right, primary peak at $\nu = 6.464$ GHz (see table 2).

However, when operated with very high input power, the multi-modality disappears and a sharp Lorentzian peak is visible (see figure 8a). The peak in this figure is centered at $\nu = 6.493$ GHz whereas the primary peak in figure 8b is centered around $\nu = 6.464$ GHz.

This shows that indeed there is a second system, the qubit, that is coupled to the cavity and which reacts on the microwave input power.

The high input power seems to saturate the influence of the qubit on the readout frequency of the cavity (also shown in [5]). Therefore figure 8a shows the uncoupled cavity and $\nu = 6.493$ GHz is the uncoupled (bare) cavity frequency.

For a high number of photons, the cavity term in the Jaynes-Cummings Hamiltonian (eq. 11) dominates the interaction which is $\propto g$. Therefore the higher energy states of the harmonic oscillator crowd out the influence of the qubit.

4.2 Coil sweep

The analysis of the resonance frequencies for a certain coil voltage only gives a limited understanding of the cavity-qubit interaction. From section 2.1.2 we understand that the applied external voltage leads to a shift in the qubits resonance frequency.
A sweep through frequency and coil voltages would therefore also show the cavity-qubit system in different regimes (resonant and dispersive).
Figure 9 resembles the theoretical prediction illustrated in fig. 2 and shows how the interaction regimes recur periodically due to the $|cos|$ dependence of the qubits frequency on external voltage.

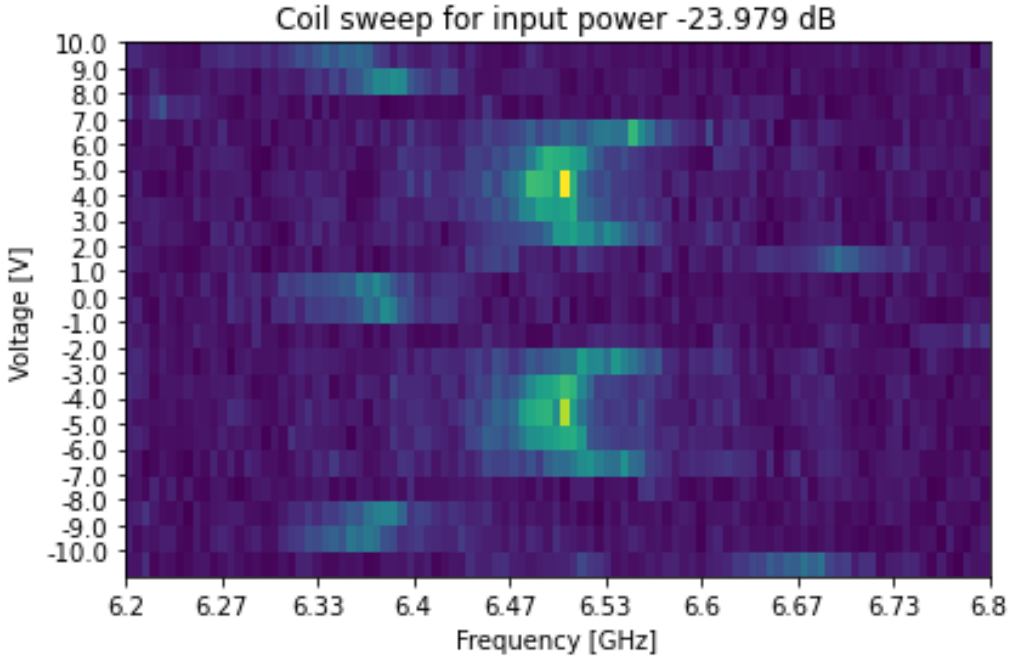

Figure 9: Two dimensional sweep of the cavity drive frequency and the voltage applied to the magnetic coil for input power -23.979 dB. The x-axis shows the frequency sweep $\nu \in [6.4, 6.6]$ GHz and the y-axis the voltage sweep $V \in [-10, 10]$ V.

The goal of this experiment will be to obtain an estimate for the coupling strength g. This can be done if we analyse the resonant regime or equivalently the avoided crossing region in the coil sweep.

4.2.1 Observations

To obtain useful data for the avoided crossing region, the voltage interval was chosen to be $V \in [-7.4, -6.6]$ V in steps of 50 mV. The frequency sweep was conducted for frequencies $\nu \in [6.4, 6.6]$ GHz in steps of 2 MHz.
The raw data of the *LabView*-based measurement framework was imported and digitized with Python. This was done by a color-coded matrix: each amplitude corresponds to a color. The color coding here used light green for high intensities and blue for low intensities. The results are displayed for increasing input power below.

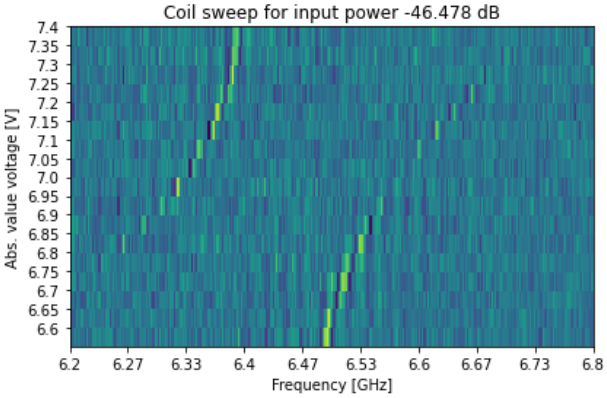

(a) Coil sweep for input power −66.478 dB

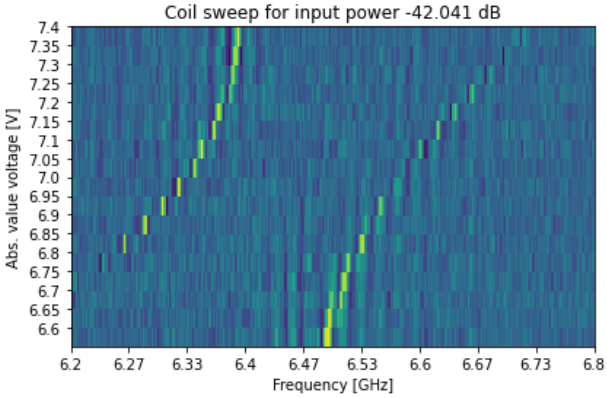

(b) Coil sweep for input power −42.041 dB

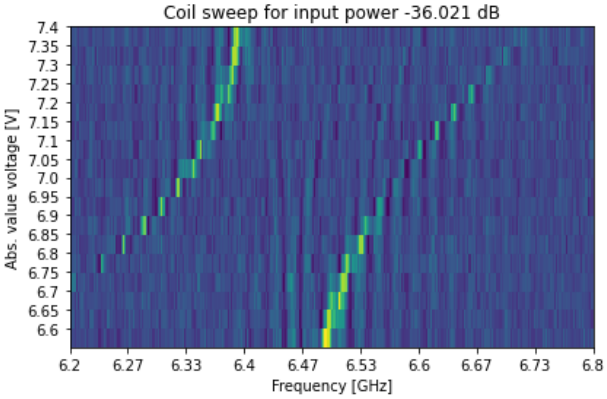

(c) Coil sweep for input power −36.021 dB

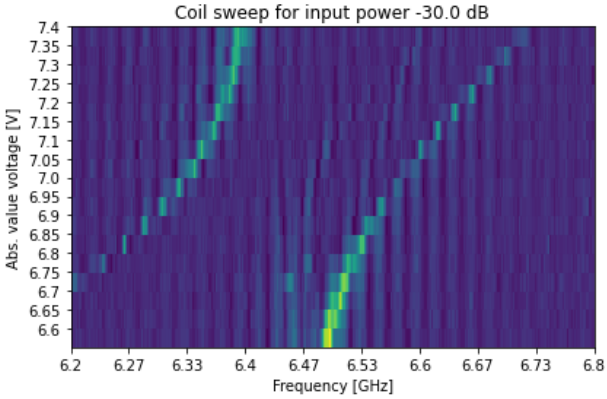

(d) Coil sweep for input power −30 dB

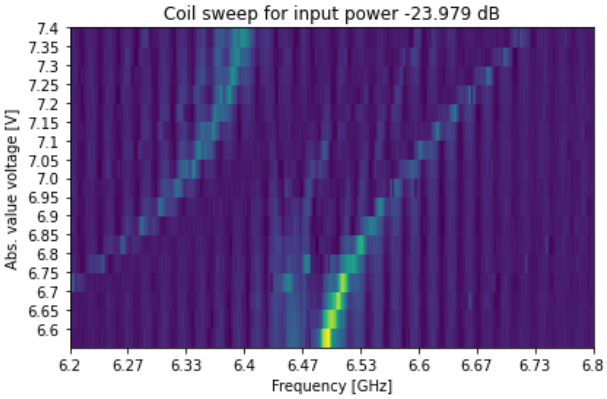

(e) Coil sweep for input power −23.979 dB

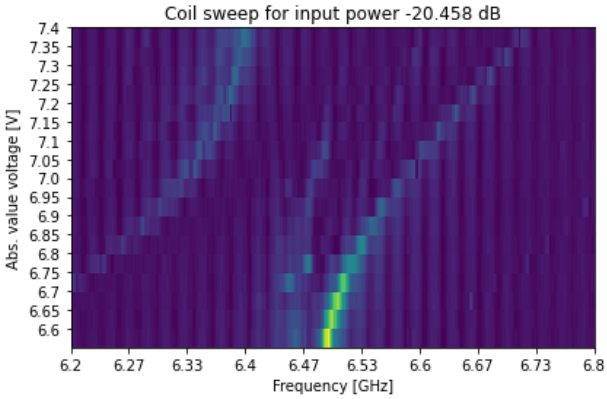

(f) Coil sweep for input power −20.458 dB

Figure 10: Two-dimensional frequency-voltage sweep for different input powers.

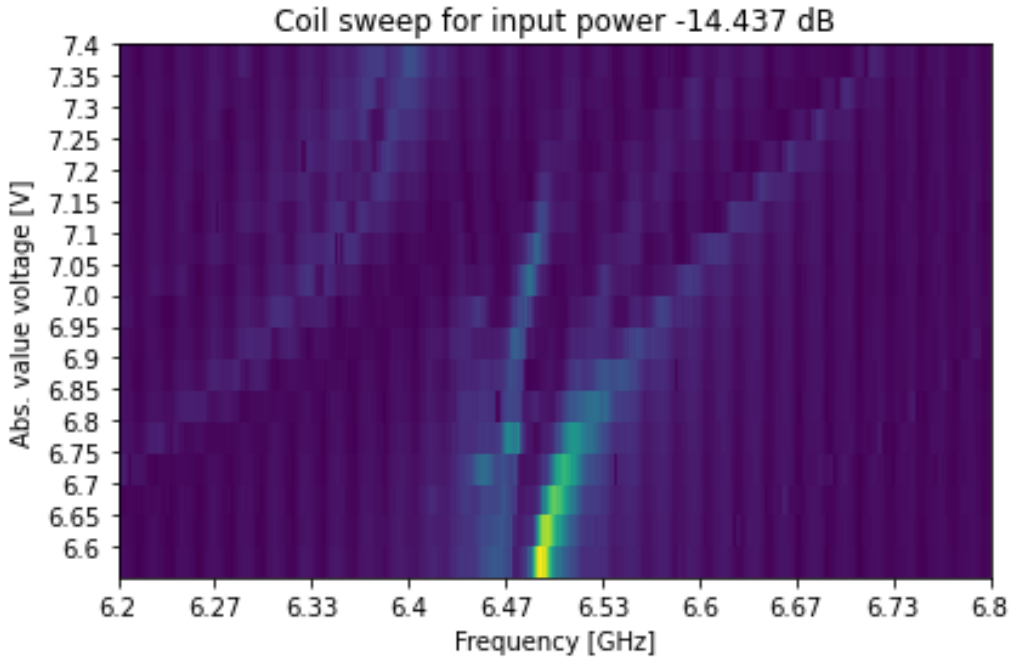

Figure 11: Coil sweep for input power -14.437 dB

4.2.2 Analysis

The observations all show the behaviour of two cavity transmission branches. In order to calculate the coupling strength g, a mathematical understanding and modelling of the avoided crossing region has to be established.

In section 2.2 the eigenenergies of the Jaynes-Cummings Hamiltonian have been defined (see equation 13). Assuming that the avoided crossing takes place in the resonant regime (i.e. $\Delta = 0$), the two branches become:

$$E_{+,n} = \hbar\omega_r n + \frac{\hbar}{2}\sqrt{4g^2 n}$$
$$E_{-.n} = \hbar\omega_r n - \frac{\hbar}{2}\sqrt{4g^2 n}$$

Hence we have an energy spacing of

$$\Delta E = 2g\hbar\sqrt{n} \tag{20}$$

which is equivalent to a minimal frequency spacing of

$$\Delta\nu = 2g \tag{21}$$

for one photon in the cavity ($n = 1$).

Graphical analysis

With this approximation a preliminary graphical analysis of the data can be made. Since the minimal distance between the frequency branches corresponds to a spacing of $2g$, a graphical estimate for g can be determined which in turn can be used as fitting guess for an analytical fit.

For that a function `shortest_dist` (see Appendix B.1) was written that extracts the intensity peaks of the two frequency branches and returns their position and an estimate for g, namely the shortest distance between all pairs.

Figure 10a and its extracted peaks are plotted together in figure 12 below.

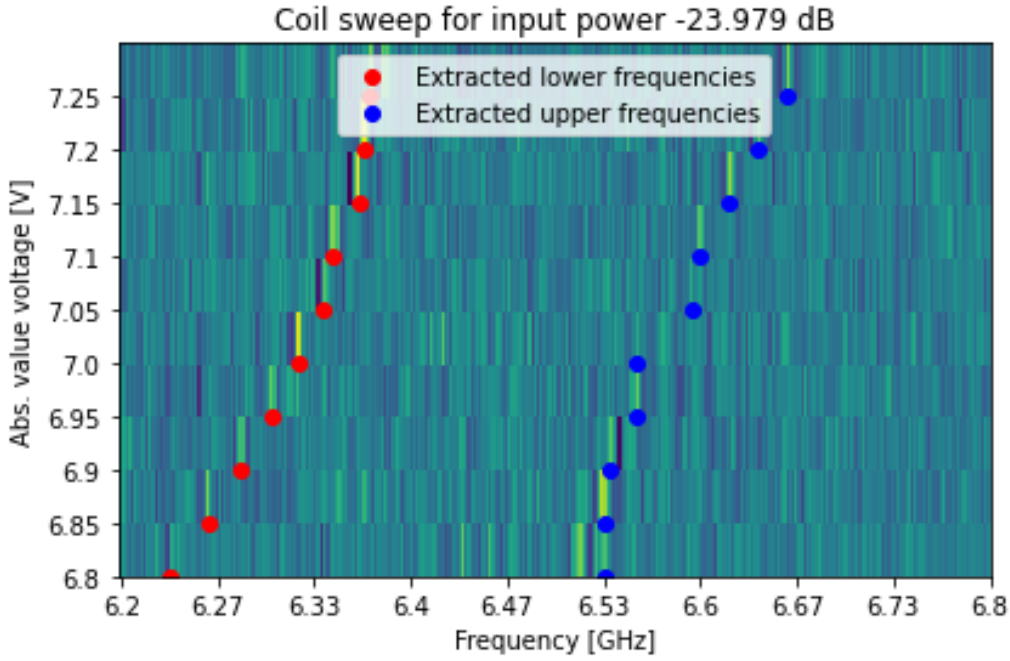

Figure 12: Coil sweep for input power -23.979 dB and extracted intensity peaks for the coil sweep. Note that the voltages are given in absolute values. The correspondence of the data and the extracted peaks is very strong. We see however, that for the high frequency branch (right branch) there are regions where the extracted peaks do not exactly corresponds to the data.

It is important to note that not the whole voltage interval is considered for the analysis. For voltages higher than -6.8 V the noise near the uncoupled cavity resonance frequency ($\nu = 6.493$ GHz) is very high. The distance between the two branches for these voltages is also never minimal. Therefore only the voltages with absolute value above 6.8 V are considered.

The graphical estimates for g are listed below.

Table 3: Graphical estimates for the coupling strength g for different linear input power. An error was attributed to the distance measurement since the frequency spacing is not infinitely fine and therefore gives room for ambiguity.

Input power $[V^2/\Omega]$	g [GHz]
4.5×10^{-10}	(0.117 ± 0.001)
1.25×10^{-7}	(0.12 ± 0.001)
5.00×10^{-7}	(0.121 ± 0.001)
2.00×10^{-6}	(0.124 ± 0.001)
8.00×10^{-6}	(0.126 ± 0.001)
1.80×10^{-5}	(0.124 ± 0.001)
7.20×10^{-5}	(0.125 ± 0.001)

These results can be plotted and fitted to analyse possible trends. Since the signal input power is proportional to the number of photons in the cavity, we can assume a $\sqrt{}$-dependence of g on the linear signal input (see eq. 20).
The corresponding fitting function therefore reads:

$$f(x) = x^{1/a} * b + c \tag{22}$$

The fit to this function results gives an estimate $a_{graphical} = (139.953 \pm 1900.425)$. The graphical result is therefore far away from the anticipated square-root dependence. This is shown in fig. 13.

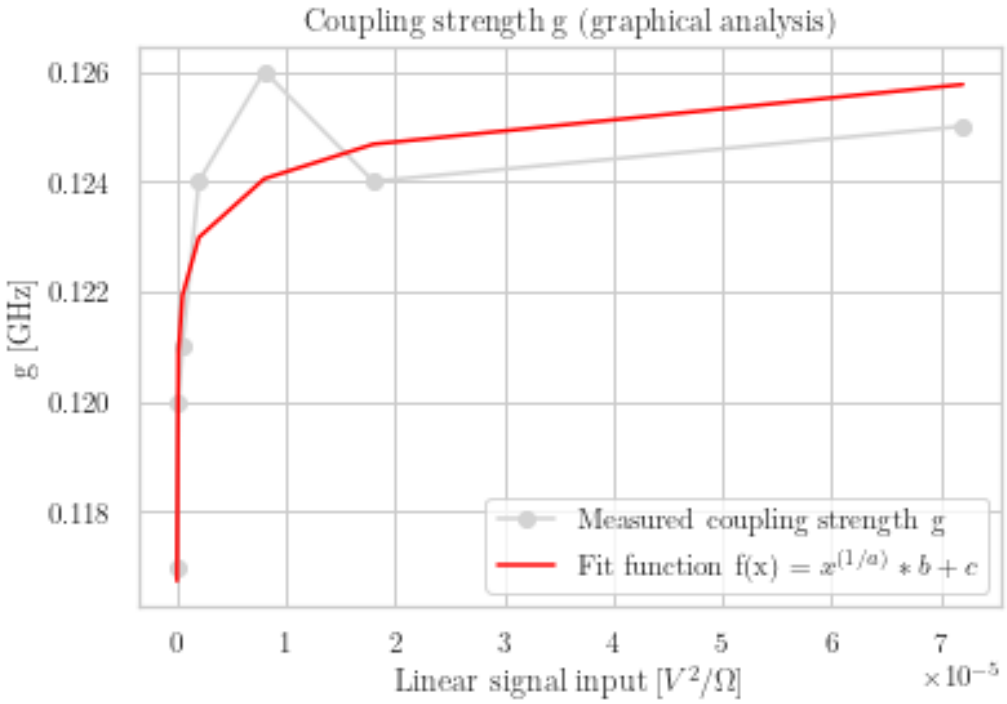

Figure 13: Coupling strength g against linear signal input. Data from table 3.

Mathematical analysis

The graphical analysis however remains a crude estimation for g since there is no exact correspondence between extracted peaks and data. A more subtle analysis of the avoided crossing and energy splitting can be made by considering the interaction Hamiltonian for the two-level system.

Let's consider the following simple model: a two-level system with zeroth-order states $|\psi_a\rangle$ (with eigenfrequency f_a) and $|\psi_b\rangle$ (with eigenfrequency f_b). The zeroth-order, uncoupled Hamiltonian then reads [9]:

$$\hat{H}_0 = |\psi_a\rangle\, f_a\, \langle\psi_a| + |\psi_b\rangle\, f_b\, \langle\psi_b| \tag{23}$$

Additionally we can construct a coupling Hamiltonian:

$$\hat{V} = |\psi_a\rangle\, g\, \langle\psi_b| + |\psi_b\rangle\, g\, \langle\psi_a| \tag{24}$$

We therefore get the full Hamiltonian as:

$$\hat{H} = \begin{pmatrix} f_a & g \\ g & f_b \end{pmatrix} \tag{25}$$

Now we can make an assumption as to how the frequencies of the two states depend on the external voltage Φ. We assume a linear dependence and have:

$$f_a = \Phi c_a + f_{a,0}$$
$$f_b = \Phi c_b + f_{b,0}$$

Here c_i is some constant and $f_{i,0}$ the center frequency. In this case, $f_{i,0}$ corresponds to the mean frequency of each frequency branch.

The function `avoided_crossing_direct_coupling` incorporates the above theory (see Appendix B.2)

The eigenfrequencies (i.e. eigenvalues) of $\hat{H}$ are the frequencies

$$f_\pm = \frac{f_a + f_b}{2} \pm \sqrt{(\frac{f_a - f_b}{2})^2 + g^2} \tag{26}$$

Now that we understand the model underlying the function `avoided_crossing_direct_coupling`, we can use it as a fitting function. The coupling strength g and its standard deviation for the different input powers are displayed in table 4. As an example, the fitted frequency branches for input power -23.979 dB are plotted together with the raw data in figure **??**.

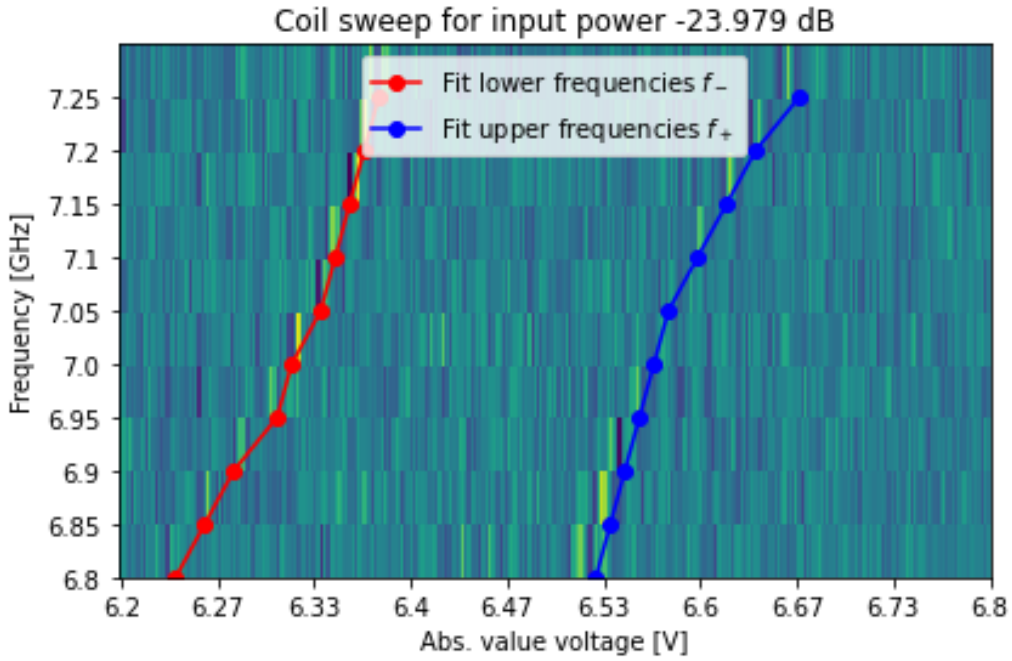

Figure 14: Fitted frequency branches f_- and f_+ of the color-coded coil sweep for input power -23.979 dB.

Table 4: Fitted parameters g and corresponding standard deviations for different input power.

Input power $[V^2/\Omega]$	g [GHz]
4.50×10^{-10}	(0.122 ± 0.0018)
1.25×10^{-7}	(0.122 ± 0.0012)
5.00×10^{-7}	(0.122 ± 0.0011)
2.00×10^{-6}	(0.123 ± 0.002)
8.00×10^{-6}	(0.125 ± 0.0013)
1.80×10^{-5}	(0.125 ± 0.0012)
7.20×10^{-5}	(0.129 ± 0.0023)

With these result we can again plot the relation g to input power and fit it to a square-root function (see eq. 22).

For the model analysis we obtain a fitting parameter $a_{model} = (2.095 \pm 0.466)$ which strongly corroborates the theory of a square-root dependece of g on the input power depicted in eq. 20. The fit can be seen in fig. 15.

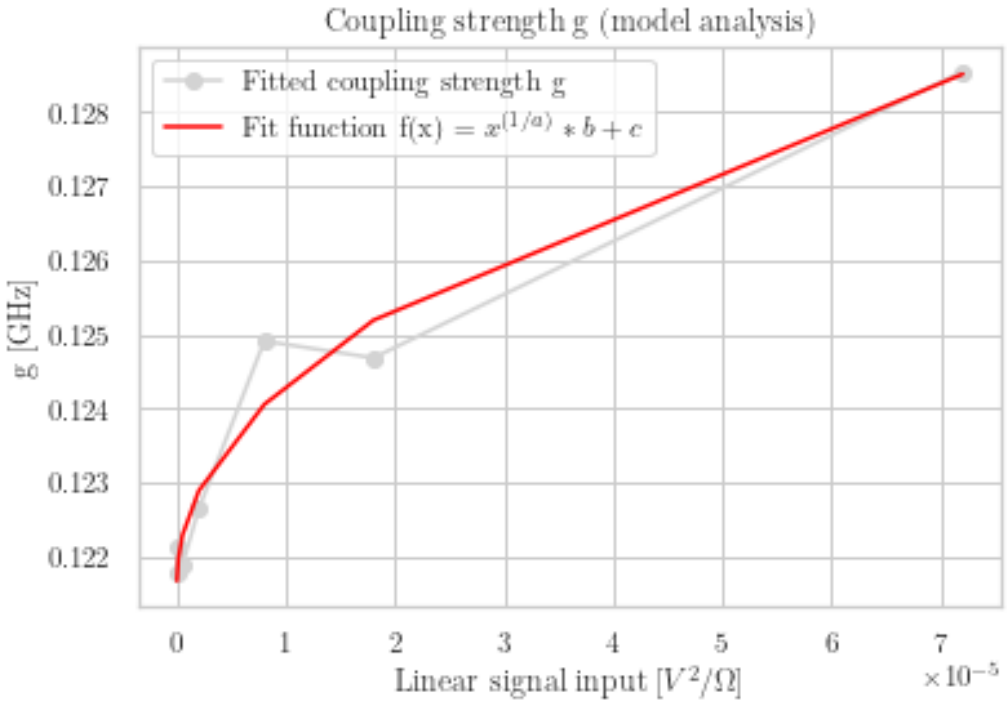

Figure 15: Coupling strength g against linear signal input. Data from table 4.

5 Conclusion

The experiment circuit QED has been an extraordinary chance to investigate quantum coupling.
In the cavity spectroscopy (section 4.1) we found that the coupling of cavity and qubit depends on the input power. For very high input power the qubit seems to be saturated and does not influence the cavitiy resonance frequency anymore.
In the coil sweep experiment (section 4.2) we were able to obtain an estimate for the coupling strength via a graphical and mathematical analysis and showed a how it depends on the signal input.

For future experiments it might be useful to establish the single photon regime ($n = 1$) such that more precise assumption can be made.
We could also infer the number of photons inside the cavity with the known dependence to g.

Appendices

A Appendix A

	Classic Mechanical	Classic Electronic	Quantum Mechanical	Quantum Electronic
Displacement	x	Φ	$\hat{x}$	$\hat{\Phi}$
Flow	p	Q	$\hat{p} = -i\hbar\frac{d}{dx}$	$\hat{Q} = -i\hbar\frac{d}{d\Phi}$
Force Proportionality	m	C	m	C
Restoring Proportionality	k	$\frac{1}{L}$	k	$\frac{1}{L}$
Resonant Frequency	$\omega = \sqrt{\frac{k}{m}}$	$\omega = \frac{1}{\sqrt{LC}}$	$\omega = \sqrt{\frac{k}{m}}$	$\omega = \frac{1}{\sqrt{LC}}$
Commutation Relations	-	-	$[\hat{x}, \hat{p}] = i\hbar$	$\left[\hat{\Phi}, \hat{Q}\right] = i\hbar$

Figure 16: Relation between classical and electric harmonic oscillator in both the quantum and classical form.[10]

B Appendix B

B.1 Shortest distance

```
import numpy as np

### Find shortest distance

cut_off = 45  ### Determine cutoff from center to avoid noise

def shortest_dist(mod_mat, freq_start, freq_end, freq_steps, volt_start,
                  volt_end, volt_steps, good_start, good_end):

    nr_of_volt_measurements = np.arange(volt_start, volt_end, volt_steps).size
```

```
    max_first_slice = max(mod_mat[0])

    pos_max_first = np.where(mod_mat[0] == max_first_slice)[0][0]

    freq_max_first = np.linspace(6.2e9, 6.8e9, 301)[pos_max_first]

    distances = []

    pairs = []

    for i in range(good_start, nr_of_volt_measurements - good_end):

        max_global = max(mod_mat[i])

        pos_max_global = np.where(mod_mat[i] == max_global)[0][0]

        freq_max_global = np.linspace(6.2e9, 6.8e9, 301)[pos_max_global]



        max_right = mod_mat[i][pos_max_first + 20:301].max()

        pos_max_right = np.where(mod_mat[i] == max_right)[0][0]

        freq_max_right = np.linspace(6.2e9, 6.8e9, 301)[pos_max_right]

        max_left = mod_mat[i][0:(pos_max_first - cut_off)].max()

        pos_max_left = np.where(mod_mat[i] == max_left)[0][0]

        freq_max_left = np.linspace(6.2e9, 6.8e9, 301)[pos_max_left]

        pos_max1 = np.where(mod_mat[i] == max_left)[0][0]
        pos_max2 = np.where(mod_mat[i] == max_right)[0][0]
```

```
            pairs.append((pos_max1, pos_max2))

            dist = np.abs(np.linspace(freq_start, freq_end, freq_steps)[pos_max2] -
                np.linspace(freq_start, freq_end, freq_steps)[pos_max1]) / 10**9



            distances.append(dist)



    shortest_dist = min(distances)

    pos_shortest_dist = distances.index(shortest_dist)



    points = [pos_max1, pos_max2]

    g = 0.5 * distances[pos_shortest_dist]

    return pairs, g
```

B.2 Avoided crossing

```
def avoided_crossing_direct_coupling(flux, f_center1, f_center2,
                                     c1, c2, g):
    """
    Calculates the frequencies of an avoided crossing for the following model.
        [f_1, g ]
        [g,  f_2]

    f1 = c1*flux + f_center1
    f2 = c2*flux + f_center2
```

```
    flux: is the array of voltages
        Data that you want to fit is the array (len(voltages, 2)) of frequencies corresp

    g:  the coupling strength

    """



    frequencies = np.zeros([len(flux), 2])

    for kk, dac in enumerate(flux):
        f_1 = dac * c1 + f_center1
        f_2 = dac * c2 + f_center2

        matrix = [[f_1, g],
                  [g, f_2]]
        frequencies[kk, :] = np.linalg.eigvalsh(matrix)[:2]
    return frequencies
```

References

[1] A. Blais et al. "Circuit quantum electrodynamics". In: *Reviews of modern physics* 93 (2021).

[2] A. Wallraff et al. "Strong coupling of a single photon to a superconducting qubit using circuit quantum electrodynamics". In: *Nature* 431 (2004), pp. 162–167.

[3] J.M. Fink et al. "Climbing the Jaynes-Cummings ladder and observing its nonlinearity in a cavity QED". In: *Nature* 454 (2008), pp. 315–318.

[4] Pedram Roushan et al. *Quantum Circuits*. URL: https://phsites.technion.ac.il/qst2019/wp-content/uploads/sites/50/2019/09/Pedram_Roushan_Lecture1_Technion_Summer_School_2019_Quantum_Circuits1.pdf. (accessed: 19.11.2021).

[5] Reed et al. "High-Fidelity Readout in Circuit Quantum Electrodynamics Using the Jaynes-Cummings Nonlinearity". In: *Physical Review Letters* 105 (2010), pp. 17360-1 - 17360–4.

[6] Johannes Fankhauser. "Frequency-tunable Transmon qubit in a 3D copper cavity". In: *ETH Zurich Semester thesis* (2016).

[7] Anders Kringhoj. *Exploring the Semiconducting Josephson Junction of Nanowire-based Superconducting Qubits*. URL: https://nbi.ku.dk/english/theses/phd-theses/anders-kringhoej/Anders_Kringhoej_PhD.pdf. (accessed: 19.11.2021).

[8] Stephanie Miller. "A tunable 20 GHz transmon qubit in a 3D cavity". In: *ETH Zurich Semester thesis* (2018).

[9] Andrej Tokmakoff. *Two-Level Systems*. URL: https://chem.libretexts.org/Bookshelves/Physical_and_Theoretical_Chemistry_Textbook_Maps/Time_Dependent_Quantum_Mechanics_and_Spectroscopy_(Tokmakoff)/02%3A_Introduction_to_Time-Dependent_Quantum_Mechanics/2.03%3A_Two-Level_Systems. (accessed: 12.11.2021).

[10] Theo Walter. *Quantum Information Theory Notes*. URL: https://qudev.phys.ethz.ch/static/content/QSIT14/QSITNotes.pdf. (accessed: 3.11.2021).

[11] Wikipedia. *Jaynes-Cummings Modell*. URL: https://de.wikipedia.org/wiki/Jaynes-Cummings-Modell. (accessed: 19.11.2021).